ARTICLE

Porous Thin Films of Functionalized Mesoporous Silica Nanoparticles

Johannes Kobler and Thomas Bein*

Department of Chemistry and Biochemistry and Center for NanoScience (CeNS), University of Munich, Butenandtstr. 5-13 (E), D-81377 Munich, Germany

ABSTRACT The synthesis of extremely small mesoporous silica nanoparticles *via* a specific co-condensation process with phenyl groups is demonstrated. The suspensions are ideally suited for the production of nanoscale thin films by spin-coating. Thanks to the small particle size and the resulting low surface roughness, the films show excellent optical qualities and exhibit good diffusion properties and a highly accessible pore system. The availability of such homogeneous porous thin films made it possible to use ellipsometric porosimetry (EP) as a convenient method to determine the effective porosity of the films on their original support without destroying it. It was possible to record sorption isotherms of the thin films with ellipsometry and to correlate the data with nitrogen sorption data of dried powders of the same material. The thin films showed very low refractive indices of around 1.2.

KEYWORDS: colloidal · nanoparticle · mesoporous silica · thin film · ellipsometry · sorption

Porous materials in the nanometer range already attract a great deal of interest in many fields of science and technology. Especially in terms of colloidal suspensions, these materials are promising candidates for applications such as gas sensing, host−guest chemistry, drug delivery, and coatings in the semiconductor industry. The preparation of monodisperse, stable colloidal suspensions of mesoporous silica particles has been recently developed.[1,2] As reported previously, the introduction of functional groups during the co-condensation reaction can have a great influence on the particle shape and size.[3] We have recently reported that the synthesis with phenyltriethoxysilane led to particles with a smallest diameter of only 50 nm.[4] Additionally, the phenyl-modified particles are thermally more stable, easy to characterize, and tend to peptize (disperse) more easily due to their sterically demanding and inert aromatic rings.

By further decreasing the diameter of these mesoporous silica spheres, their scattering ability for visible light is also drastically decreased. If the size of the particles falls below about 1/10 of the wavelength of the incoming light (0.1λ), their scattering ability can be described with the Rayleigh scattering theory. The colloidal suspensions thus show optical transparency when the particle size is small enough. Due to this optical transparency, such nanoparticles would allow spectroscopic investigations of physical processes or chemical reactions in a confined space. Furthermore, it is possible to encapsulate sensitive dyes[5−8] or to facilitate the dispersion of the particles in certain media. Modifying the spheres with appropriate functionalities such as caps or fluorescence markers would make them interesting candidates for drug delivery[5,9] or would permit observing their way into a cell.[10,11] Another very promising area of application is thin film technology.[12,13] The synthesis of mesoporous thin films is often achieved with the so-called "evaporation induced self-assembly" (EISA) process.[14] The EISA process for mesoporous silica thin films starts with a homogeneous solution of silica precursor and surfactant prepared in ethanol/water with an initial surfactant concentration much below the critical micelle concentration.[14] Upon dip-coating or spin-coating, the preferential evaporation of ethanol concentrates the surfactant and silica species. The progressively increasing surfactant concentration drives self-assembly of silica-surfactant micelles and their further organization into liquid-crystalline mesophases. This approach represents a versatile strategy for the formation of mesoporous silica and other oxide thin films with different pore sizes, pore topologies, and elemental composition.[15]

However, there are several issues that suggest the development of complementary strategies. The precursor is normally

*Address correspondence to bein@lmu.de.

Received for review August 8, 2008 and accepted September 25, 2008.

Published online November 25, 2008.
10.1021/nn800505g CCC: $40.75

© 2008 American Chemical Society

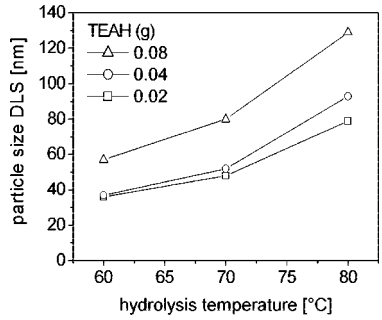

Figure 1. Initial particle size (DLS) of samples CMS-P26−CMS-P88.

highly acidic, which can cause problems on sensitive substrates. Removal of the template by extraction or calcination might also be critical. If the surfactant is removed thermally, cracks can occur in thicker films, and it is known that the humidity has a great influence on the film formation. Thus, if the orientation of the pores is less important, the alternative preparation of thin films with mesoporous nanoparticles can address several of these issues. It is believed that a porous thin film made of porous nanoparticles can exhibit improved diffusion properties and a highly accessible pore system.[16] Additionally, one can work with stable suspensions of already extracted nanoparticles, thus ensuring easy handling and good reproducibility. The coating of sensitive substrates is facilitated due to the mild conditions. Control over the thickness can be attained by varying the concentration or by multiple step coating. Finally, the material can be more easily characterized if bulk samples are available. The synthesis of completely transparent suspensions even after template extraction would therefore be a great improvement for the formation of homogeneous thin films with a low surface roughness. Especially for the formation of multilayers, it is advantageous if the film is very smooth. Otherwise the defects on the surface are transmitted and amplified with every following coating step. Furthermore, the availability of such homogeneous porous thin films makes it possible to use ellipsometric porosimetry as an analysis method. This method has a set of advantages compared to conventional sorption methods, which are specified in a work of Eslava *et al.*[17]

For an accurate determination of sorption isotherms of porous coatings *via* gravimetric or volumetric methods, an extremely sensitive device is needed. The tiny amount of porous material and the weight increase due to adsorption in the thin film can be detected with a surface acoustic wave (SAW) device or a quartz crystal microbalance (QCM). In both cases, the coating has to be applied to the measuring device itself, which might have an influence on properties such as the orientation of the crystals, the presence of grain boundaries, and the film thickness. Scraping films off from their supports and collecting a sufficient quantity of powdery sample for a conventional determination is a drastic intervention. The determination of sorption isotherms of a thin film *via* ellipsometric porosimetry (EP) is therefore a convenient method to determine the effective porosity and pore size distribution of a thin film on its original support without destroying it.

Thus, the aim of this work was the synthesis of monodisperse colloidal suspensions of porous nanoparticles with a particle size small enough for the preparation of homogeneous thin films. Additionally, the porosity of the final thin films was determined with different methods.

RESULTS AND DISCUSSION

The synthesis results are in good accordance with the expectations based on the work of Stöber[18] and LaMer.[19] A first important variable is the amount of precursor added to the synthesis. In a certain range, decreasing the amount of precursor can reduce the size of the final particles. According to Stöber, the particle size distribution passes a maximum when the concentration is varied because the concentration of precursor influences not only the growth of the seeds but also the nucleation rate and thus the number of initial seeds. Since high yield is a priority, it is more interesting to choose other options for a successful downsizing. The experiments show that the final particle size in the resultant suspensions (CMS-P26−CMS-P88) is dependent on the amount of added TEAH and the reaction temperature. In Figure 1, the hydrodynamic diameter of all samples is shown (CMS-P**86** stands for synthesis with 0.0**8** g of TEAH at **6**0 °C).

With increasing temperature and amount of catalyst (TEAH), the hydrolysis of the precursor and conden-

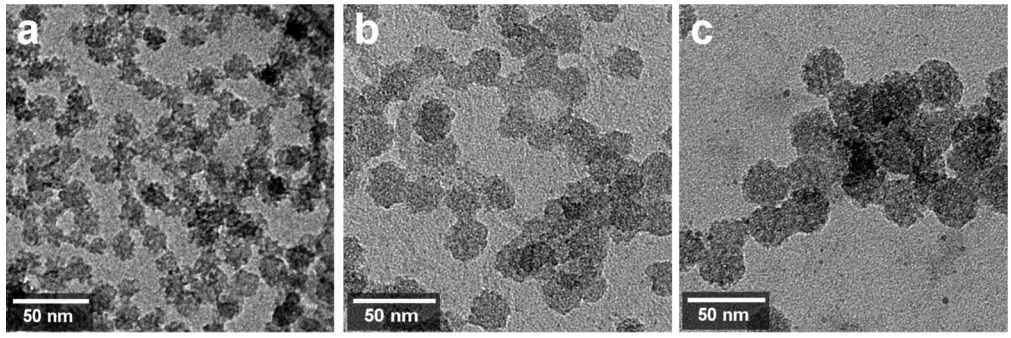

Figure 2. Electron micrographs (TEM) of samples (a) CMS-P86, (b) CMS-P87, and (c) CMS-P88.

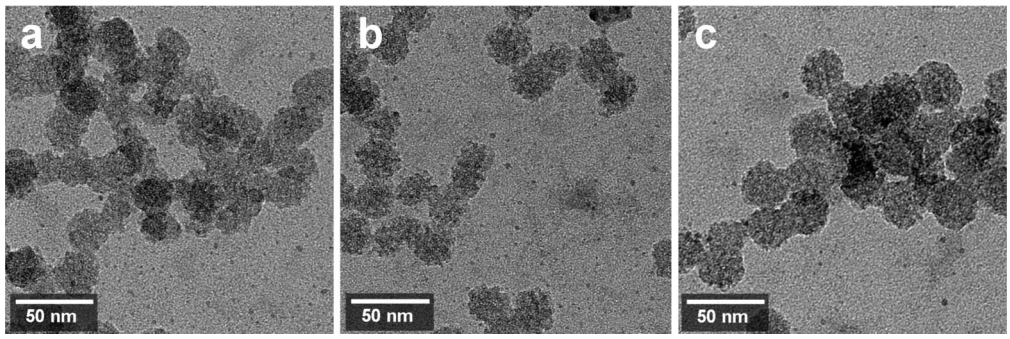

Figure 3. Electron micrographs (TEM) of samples (a) CMS-P28, (b) CMS-P48, and (c) CMS-P88.

sation of the nanoparticles is supported and the reaction is faster. In this specific range, these changes apparently promote the growth rate more than the nucleation rate, resulting in bigger particles. Figure 2 shows micrographs (TEM) of samples synthesized at different temperatures with the same amount of TEAH (CMS-P8*y*). The difference in size can be clearly seen; the particles that formed at 60 °C (CMS-P86) show the smallest diameter of only 15 nm. At 70 and 80 °C, the diameter reaches 25 and 30 nm, respectively.

In agreement with DLS data, TEM also shows that the variation of the amount of catalyst TEAH at a constant reaction temperature (80 °C, CMS-*x*8) has an influence on the particle size (Figure 3). The difference is less pronounced, but the general tendency can be confirmed. The diameter varies between 22 (CMS-P28), 25 (CMS-P48), and 30 nm (CMS-P88) if the quantity of TEAH is increased.

Table 1 shows a comparison of DLS and TEM data for selected particle sizes. The divergence in hydrodynamic diameter in DLS (36−130 nm) and discrete particle size in TEM (15−30 nm) could be explained with a higher degree of agglomeration at higher temperatures.

The above findings made it possible to synthesize colloidal suspensions of functionalized, mesoporous silica nanoparticles with a very small particle size between 15 and 30 nm. As the scattering intensity (*I*) of light strongly decreases with smaller particles size ($I \sim \text{radius}^6$), the suspensions with the smallest diameter (~15 nm) are completely clear (Figure 4).

When reaching a certain size, separating particles with centrifuges becomes difficult, as the effective gravitational force is dependent on the mass of the particles. An elegant method to overcome this problem is the flocculation of the particles. Therefore, acidified ethanol was added to the aqueous colloidal suspension leading to a cloudy suspension of agglomerated particles. The particles then could be separated from the solution by centrifugation and were purified in the following steps. The final gelatinous sediment can be completely redispersed in ethanol, leading to transparent colloidal suspensions with almost exactly the initial particle size distribution in DLS. Figure 5 shows the mean hydrodynamic diameter of CMS-P86 before and after template extraction. The polydispersity index (PDI) of all suspensions was below 0.2. The suspensions with a diameter below 40 nm are completely transparent to the visible part of the light and show nearly no scattering.

In transmission electron microscopy (TEM), the diameter of the individual particles can be specified as significantly smaller (by a factor of 3) than that in dynamic light scattering. Figure 6 shows micrographs of CMS-P86 with an average particle diameter of about 20 nm. The size distribution of the discrete particles is

TABLE 1. Particle Size (DLS, TEM) and Maximum in Interparticle Porosity (N_2 Sorption)

sample	hydrodynamic diameter (DLS)	diameter (TEM)	maximum interparticle porosity
CMS-P88	130	30	16
CMS-P48	95	25	14
CMS-P28	80	22	12
CMS-P87	80	25	14
CMS-P86	60	15	9

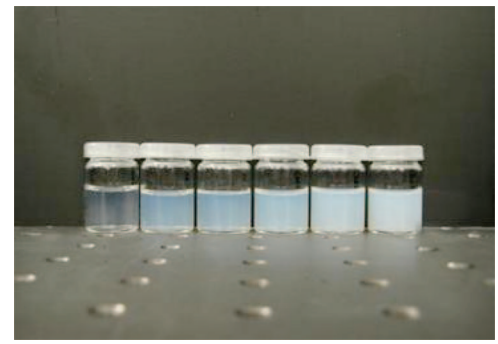

Figure 4. Scattering of the initial colloidal suspensions containing particles with different diameters (DLS) in the range between about 40 to 130 nm (left to right: CMS-P27, -P86, -P28, -P87, -P48, -P88, see Table 1 and Figure 1).

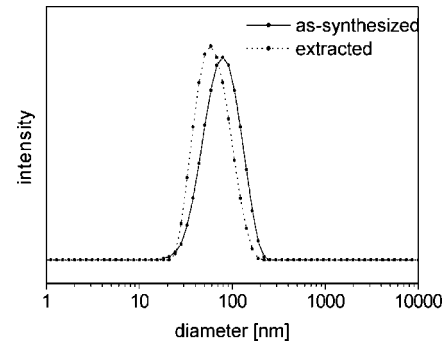

Figure 5. Hydrodynamic diameter of CMS-P86 before and after template extraction.

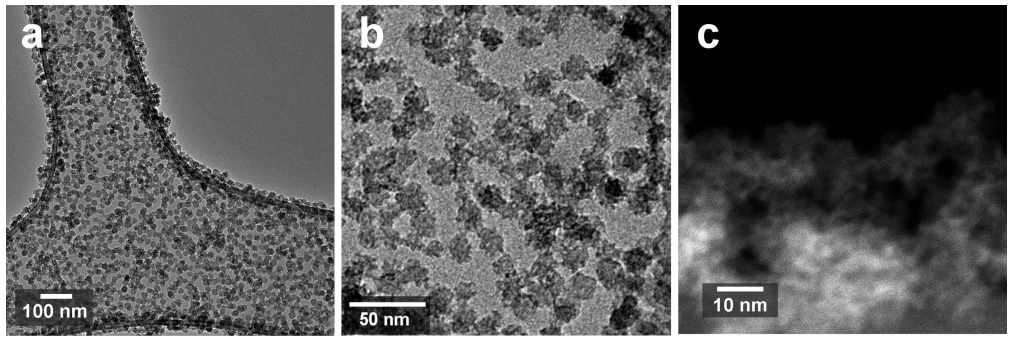

Figure 6. TEM micrographs of CMS-P86 (right: HAADF-STEM).

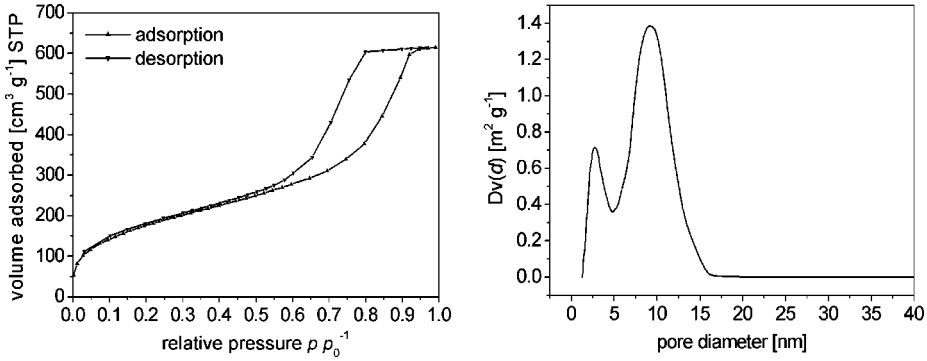

Figure 7. N_2 sorption data of dried, extracted CMS-P86.

very narrow. High-resolution images clearly show the porous nature of the functionalized particles.

In order to investigate the sorption properties of the porous nanoparticles, the ethanolic suspensions were dried at 60 °C. The resulting solids were colorless and transparent, consisting of small platelets with about 1 mm diameter. Despite its dense appearance, the material has a high specific surface area of 640 $m^2 g^{-1}$ as well as a high pore volume (0.95 $cm^3 g^{-1}$) in the case of CMS-P86. DFT calculations resulted in a bimodal pore size distribution (Figure 7).

The first peak at 2.7 nm due to templated mesopores is in the expected range for functionalized mesoporous silica templated by hexadecyltrimethylammonium ions. The second peak around 10 nm reflects the textural porosity of the material. It is a widely accepted concept that an inscribed sphere between adjacent spheres is an approximate shape for the access opening to the interstitial void space between randomly packed spheres.[20−22] Depending on the packing of the individual particles, the pore opening varies approximately between 0.2 and 0.6 times the radius of the equally sized particles. In the case of CMS-P86, this interparticle porosity is in the range between 5 and 15 nm (compare Figure 7). Thus, the expected particle size based on sorption is about 25 nm, which coincides well with the observed diameter in the TEM. With decreasing particle size, this second peak is shifted to smaller pore sizes as shown in Figure 8. The maximum of the interparticle porosity is in the expected range for all samples (see Table 1).

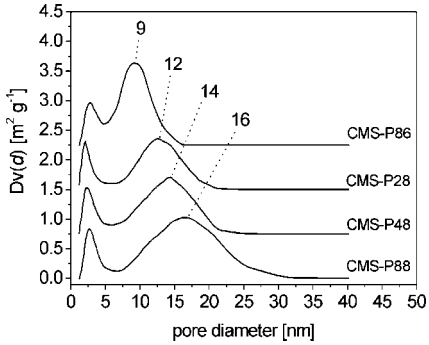

Figure 8. Pore size distribution from N_2 sorption of differently sized mesoporous particles with maximum for interparticle porosity.

Homogeneous Thin Films. The ethanolic suspensions of the template-free material are ideal candidates for the preparation of homogeneous spin-on thin films. The dry bulk material exhibits a high surface area even though it appears to be a dense solid. Thus, one can expect a

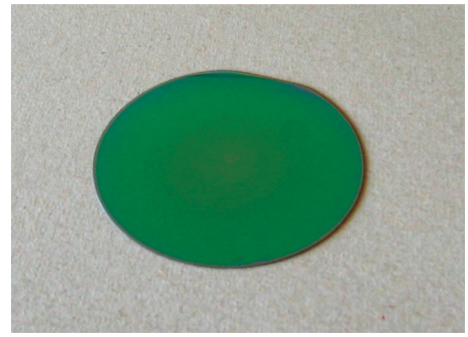

Figure 9. Thin film of CMS-P86 on a silicon wafer.

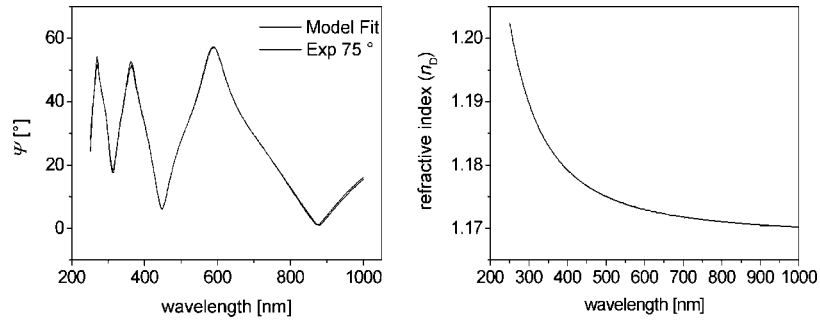

Figure 10. Ellipsometry data of a thin film of CMS-P86 in nitrogen atmosphere.

high porosity for the corresponding thin film. Figure 9 shows an image of a silicon wafer with a thin film of mesoporous functionalized silica with a thickness of 650 nm. The film was prepared by spin-coating three times with an ethanolic suspension containing 5 wt % of CMS-P86.

The film appears very homogeneous and transparent and thus has a definite interference color. Due to pronounced capillary forces occurring during the solvent evaporation, the nanoparticles are very closely packed—a phenomenon that also assists in the assembly of colloidal crystals.[23] Because of the smooth surface, no scattering is observed, which makes the films perfect candidates for ellipsometry investigations. Modeling and fitting of the data was based on the assumption that the film consists of porous nanoparticles; the model layer was designed as follows: (1) the silicon substrate is infinitely thick (1 mm); (2) a typical layer of 2 nm thermal oxide (SiO_2) is presumed; (3) the material (organically functionalized silica) is described with a Cauchy layer. Starting with a guessed film thickness of 500 nm, the subsequent fitting of the thickness and the Cauchy parameters resulted in a 650 nm thick film. As shown in Figure 10, this model layer fits exactly the experimental data.

The measurement was performed in a flow cell in a flow of nitrogen. It was repeated at different relative pressures of gaseous toluene. The adsorption affinity of the thin film can be also observed when the interference color changes due to the pore filling. The relative pressure of toluene was controlled between 0 and 0.943 ($p\ p_0^{-1}$). Plotting the refractive index of the thin film *versus* the relative pressure of toluene resulted in the isotherm shown in Figure 11.

After the templated mesopores are filled, a second step due to the filling of the interparticle porosity can be identified at a relative pressure of 0.6−0.8. The ellipsometric data are in very good accordance with powder nitrogen sorption data (Figure 12). The overlay shows the same sorption behavior for the two different adsorbates.

Applying the Lorentz−Lorenz equation for ellipsometric porosimetry (EP), a porosity of 53% is obtained for the film CMS-P86. If the total pore volume of 0.95 $cm^3\ g^{-1}$ obtained from N_2 sorption is correlated to the 53% porosity in ellipsometric data, an overall film density of 0.56 g cm^{-3} can be calculated.

CONCLUSION

In this study, we have demonstrated the synthesis of extremely small mesoporous silica nanoparticles *via* a specific co-condensation process with phenyl groups. The size of the suspended mesoporous silica spheres can be controlled in a wide range. The suspensions with a mean hydrodynamic particle diameter of about 40 nm or less were optically transparent. After extraction of the surfactant, dispersion in ethanol led to transparent colloidal suspensions. The existence of very small individual porous particles was confirmed by transmission electron microscopy (TEM) and sorption measurements. The suspensions were used for the preparation of homogeneous porous thin films by spin-coating. The films showed excellent optical qualities and could thus be char-

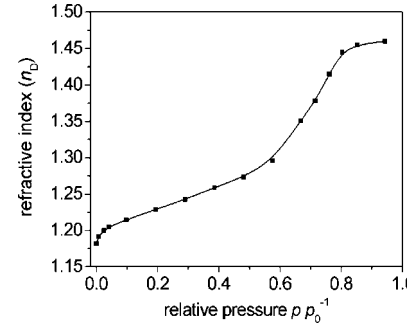

Figure 11. Ellipsometry data of a thin film of CMS-P86 in toluene vapor in a nitrogen atmosphere.

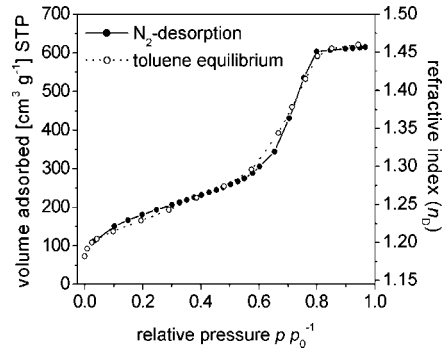

Figure 12. Overlay of a powder N_2 sorption isotherm (desorption) and a toluene isotherm (equilibrium) of a thin film recorded with ellipsometry (CMS-P86).

acterized with ellipsometry. It was possible to record sorption isotherms of the thin films with ellipsometry and to correlate the data with nitrogen sorption data of dried powders of the same material. In the future, exchange of the template is anticipated to allow control over the pore size, and molecular modification of the internal surface of the mesopores will offer numerous new functionalities of the nanoparticles and the resulting thin films.

EXPERIMENTAL SECTION

All chemicals were purchased from Sigma-Aldrich with reagent grade (98% or higher) and used without further purification. The water was deionized. In order to ensure the same conditions for all samples, the syntheses were carried out in a heatable high-throughput magnetic stirrer system (1000 rpm) in 100 mL glass test tubes (diameter = 2.5 cm). Although it is necessary that the synthesis mixture be well stirred, building of foam should be avoided in order to prevent the formation of inhomogeneities. The following solutions were prepared and used for all syntheses: **S1** (surfactant): 30.0 g aqueous solution of cetyltrimethylammonium chloride (25 wt %) and 270.0 g of deionized water. **C1** (catalyst): 1.0 g of triethanolamine (TEAH) and 9.0 g of deionized water. **P1** (precursor): 20.8 g (0.1 mol) of tetraethylorthosilicate (TEOS) and 2.4 g (0.01 mol) of phenyltriethoxysilane (PTES). **E1** (extraction): 50 g of concentrated hydrochloric acid (37% HCl) in 500 mL of ethanol. **E2** (extraction): 10 g of ammonium nitrate in 500 mL of ethanol.

Samples CMS-P*xy*. The amount of 20.0 g of **S1** and 0.20 (CMS-P2*y*), 0.40 (CMS-P4*y*), or 0.80 g (CMS-P8*y*) of **C1** was heated under stirring to 60 (CMS-P*x*6), 70 (CMS-P*x*7), or 80 °C (CMS-P*x*8). The amount of 1.60 mL of **P1** was added, and stirring was continued in the test tube for 1 h. The vessel was kept open in order to evaporate parts of the ethanol that were formed during the condensation. For a better overview, all samples are listed in Table 2.

Extraction. The resulting colloidal suspension was flocculated with 20 mL of **E1**, and the cloudy precipitate was centrifuged for 5 min at 40 000*g* (RCF). After decanting, the sediment was redispersed through vigorous stirring in 20 mL of **E2**. The clear suspension was treated for 10 min in an ultrasonic bath. After flocculating with 20 mL of deionized water, the precipitate was again centrifuged, the sediment was redispersed in 20 mL of **E1**, and again sonicated. After flocculation with 20 mL of deionized water and centrifugation, the sediment can be redispersed in ethanol, leading to a suspension of colloidal mesoporous silica (CMS) with approximately 5 wt % solid content.

Film Preparation. Thin film preparation was performed by spin-coating with an ethanolic suspension containing about 5 wt % of solid material. The substrate (silicon or glass) was coated three times at 3000 rpm (acceleration = 5000 rpm s^{-1}). In order to remove potential inhomogeneities, the transparent ethanolic suspension was filtered through a 0.2 μm syringe filter prior to spin-coating.

Characterization. Dynamic light scattering (DLS) data were collected with a Malvern Nano ZS in PMMA cuvettes at 25 °C. Transmission electron microscopy (TEM) was carried out on a FEI Titan 80-300 at an accelerating voltage of 300 kV. Samples were prepared on a Plano holey carbon coated copper grid by evaporating one droplet of diluted ethanolic suspension of the extracted material. The nitrogen sorption isotherms (77 K) were obtained using a Quantachrome NOVA 4000e surface area and pore size analyzer. Surface area calculations were made using the Brunauer–Emmett–Teller (BET) equation in the range of $p\,p_0^{-1} = 0.05$ to 0.25. Pore size distributions were determined using the DFT-method (NLDFT equilibrium model, cylindrical pores, N_2 on carbon). Ellipsometry measurements were performed with a Woollam M2000D at different angles (65, 70, and 75°) in the spectral range of 190–1000 nm. The data were fitted in the range between 250 and 1000 nm using a Cauchy-type material as model layer. Ellipsometric porosimetry measurements were carried out in a closed cell at different partial pressures at a measurement angle of 75° (see Supporting Information for further details). The recording of isotherms was performed using a homemade Labview-controlled gas mixer. Digital mass flow controllers (W-101A-110-P, F-201C, Bronkhorst High-Tech) ensured the accurate dosing of the carrier gas nitrogen and the liquid analyte, which was vaporized in a controlled evaporation and mixing element (W-101A, Bronkhorst High-Tech). Partial pressures were calculated using the van der Waals equation.

TABLE 2. Prepared Samples and Synthesis Conditions

sample	synthesis temperature	amount TEAH (g)
CMS-P26	60°C	0.02
CMS-P46	60°C	0.04
CMS-P86	60°C	0.08
CMS-P27	70°C	0.02
CMS-P47	70°C	0.04
CMS-P87	70°C	0.08
CMS-P28	80°C	0.02
CMS-P48	80°C	0.04
CMS-P88	80°C	0.08

Acknowledgment. Funding for this work from the Deutsche Forschungsgemeinschaft (SFB 486, NIM Cluster) is gratefully acknowledged. We thank Wacker Siltronic AG for the donation of silicon wafers, and S. Schmidt and M. Döblinger for the recording of electron micrographs.

Supporting Information Available: A review of how ellipsometric porosimetry is used to describe the change of the optical properties that are associated with the sorption of volatile species. This material is available free of charge *via* the Internet at http://pubs.acs.org.

REFERENCES AND NOTES

1. Moeller, K.; Kobler, J.; Bein, T. Colloidal Suspensions of Nanometer-Sized Mesoporous Silica. *Adv. Funct. Mater.* **2007**, *17*, 605–612.
2. Moeller, K.; Kobler, J.; Bein, T. Colloidal Suspensions of Mercapto-Functionalized Nanosized Mesoporous Silica. *J. Mater. Chem.* **2007**, *17*, 624–631.
3. Huh, S.; Wiench, J. W.; Yoo, J.-C.; Pruski, M.; Lin, V. S.-Y. Organic Functionalization and Morphology Control of Mesoporous Silicas *via* a Co-Condensation Synthesis Method. *Chem. Mater.* **2003**, *15*, 4247–4256.
4. Kobler, J.; Möller, K.; Bein, T. Colloidal Suspensions of Functionalized Mesoporous Silica Nanoparticles. *ACS Nano* **2008**, *2*, 791–799.
5. Sokolov, I.; Kievsky, Y. Y.; Kaszpurenko, J. M. Self-Assembly of Ultrabright Fluorescent Silica Particles. *Small* **2007**, *3*, 419–423.
6. Ren, T.-Z.; Yuan, Z.-Y.; Su, B.-L. Encapsulation of Direct Blue Dye into Mesoporous Silica-Based Materials. *Colloids Surf., A* **2007**, *300*, 79–87.
7. Laerte de Castro, F.; Santos, J. G.; Fernandes, G. J. T.; Souza de Araujo, A.; Fernandes, V. J.; Politi, M. J.; Brochsztain, S. Solid State Fluorescence of a 3,4,9,10-Perylenetetracarboxylic Diimide Derivative Encapsulated in the Pores of Mesoporous Silica MCM-41. *Microporous Mesoporous Mater.* **2007**, *102*, 258–264.
8. Wark, M.; Ganschow, M.; Rohlfing, Y.; Schulz-Ekloff, G.; Woehrle, D. Methods of Synthesis for the Encapsulation of Dye Molecules in Molecular Sieves. *Stud. Surf. Sci. Catal.* **2001**, *135*, 3292–3300.
9. Trewyn, B. G.; Giri, S.; Slowing, I. I.; Lin, V. S.-Y. Mesoporous Silica Nanoparticle-Based Controlled Release, Drug

Delivery, and Biosensor Systems. *Chem. Commun.* **2007**, 3236–3245.
10. Huang, D.-M.; Hung, Y.; Ko, B.-S.; Hsu, S.-C.; Chen, W.-H.; Chien, C.-L.; Tsai, C.-P.; Kuo, C.-T.; Kang, J.-C.; Yang, C.-S.; et al. Highly Efficient Cellular Labeling of Mesoporous Nanoparticles in Human Mesenchymal Stem Cells: Implication for Stem Cell Tracking. *FASEB J.* **2005**, *19*, 2014–2016.
11. Torney, F.; Trewyn, B. G.; Lin, V. S. Y.; Wang, K. Mesoporous Silica Nanoparticles Deliver DNA and Chemicals into Plants. *Nat. Nanotechnol.* **2007**, *2*, 295–300.
12. Chen, J. Y.; Pan, F. M.; Chang, L.; Cho, A. T.; Chao, K. J. Thermal Stability of Trimethylsilylated Mesoporous Silica Thin Films as the Ultralow-*k* Dielectric for Copper Interconnects. *J. Vac. Sci. Technol., B* **2005**, *23*, 2034–2040.
13. Innocenzi, P.; Martucci, A.; Guglielmi, M.; Bearzotti, A.; Traversa, E.; Pivin, J. C. Mesoporous Silica Thin Films for Alcohol Sensors. *J. Eur. Ceram. Soc.* **2001**, *21*, 1985–1988.
14. Brinker, C. J.; Lu, Y. F.; Sellinger, A.; Fan, H. Y. Evaporation-Induced Self-Assembly: Nanostructures Made Easy. *Adv. Mater.* **1999**, *11*, 579–585.
15. Brinker, C. J. Evaporation-Induced Self-Assembly: Functional Nanostructures Made Easy. *MRS Bull.* **2004**, *29*, 631–640.
16. Lee, U. H.; Kim, M.-H.; Kwon, Y.-U. Mesoporous Thin Films with Accessible Pores from Surfaces. *Bull. Korean Chem. Soc.* **2006**, *27*, 808–816.
17. Eslava, S.; Baklanov, M. R.; Kirschhock, C. E. A.; Iacopi, F.; Aldea, S.; Maex, K.; Martens, J. A. Characterization of a Molecular Sieve Coating Using Ellipsometric Porosimetry. *Langmuir* **2007**, *23*, 12811–12816.
18. Stober, W.; Fink, A.; Bohn, E. Controlled Growth of Monodisperse Silica Spheres in the Micron Size Range. *J. Colloid Interface Sci.* **1968**, *26*, 62–69.
19. LaMer, V. K.; Dinegar, R. H. Theory, Production and Mechanism of Formation of Monodispersed Hydrosols. *J. Am. Chem. Soc.* **1950**, *72*, 4847–4854.
20. Mason, G. A Model of the Pore Space in a Random Packing of Equal Spheres. *J. Colloid Interface Sci.* **1971**, *35*, 279–287.
21. Slobozhanin, L. A.; Alexander, J. I. D.; Collicott, S. H.; Gonzalez, S. R. Capillary Pressure of a Liquid in a Layer of Close-Packed Uniform Spheres. *Phys. Fluids* **2006**, *18*, 082104–082115.
22. Mayer, R. P.; Stowe, R. A. Packed Uniform Sphere Model for Solids: Interstitial Access Opening Sizes and Pressure Deficiencies for Wetting Liquids with Comparison to Reported Experimental Results. *J. Colloid Interface Sci.* **2006**, *294*, 139–150.
23. Juillerat, F.; Bowen, P.; Hofmann, H. Formation and Drying of Colloidal Crystals Using Nanosized Silica Particles. *Langmuir* **2006**, *22*, 2249–2257.